Are Watermarks Bugs for Deepfake Detectors? Rethinking Proactive Forensics

Xiaoshuai Wu , Xin Liao* , Bo Ou , Yuling Liu , Zheng Qin
College of Computer Science and Electronic Engineering, Hunan University, Changsha, China
{shinewu, xinliao, oubo, yuling_liu, zqin}@hnu.edu.cn

Abstract

AI-generated content has accelerated the topic of media synthesis, particularly Deepfake, which can manipulate our portraits for positive or malicious purposes. Before releasing these threatening face images, one promising forensics solution is the injection of robust watermarks to track their own provenance. However, we argue that current watermarking models, originally devised for genuine images, may harm the deployed Deepfake detectors when directly applied to forged images, since the watermarks are prone to overlap with the forgery signals used for detection. To bridge this gap, we thus propose AdvMark, on behalf of proactive forensics, to exploit the adversarial vulnerability of passive detectors for good. Specifically, AdvMark serves as a plug-and-play procedure for fine-tuning any robust watermarking into adversarial watermarking, to enhance the forensic detectability of watermarked images; meanwhile, the watermarks can still be extracted for provenance tracking. Extensive experiments demonstrate the effectiveness of the proposed AdvMark, leveraging robust watermarking to fool Deepfake detectors, which can help improve the accuracy of downstream Deepfake detection without tuning the in-the-wild detectors. We believe this work will shed some light on the harmless proactive forensics against Deepfake.

1 Introduction

Large generative models like ChatGPT and Stable Diffusion are transforming the way we communicate, illustrate, and create [Hacker *et al.*, 2023]. Despite their positive potential in applications such as entertainment, education, art, etc., we cannot neglect the negative impacts. Particularly, the photo-realistic Deepfake [Hu *et al.*, 2022], interpreted as "fake face" generated through "deep learning", has taken false messages and misleading content to a new level, thereby damaging social trust and public interest [Juefei-Xu *et al.*, 2022]. In response to this dilemma, emerging standards such as the Coalition for Content Provenance and Authenticity [C2PA, 2021] call for embedding provenance information within the released images online [Bui *et al.*, 2023]. To build Responsible AI, major tech companies, including Google and Microsoft, are also developing tools to trace the origin and identify synthetically altered or created images [Zhao *et al.*, 2023a]. It has never been more important to understand the provenance and authenticity of the images we see, helping us make informed decisions and protect ourselves from deception.

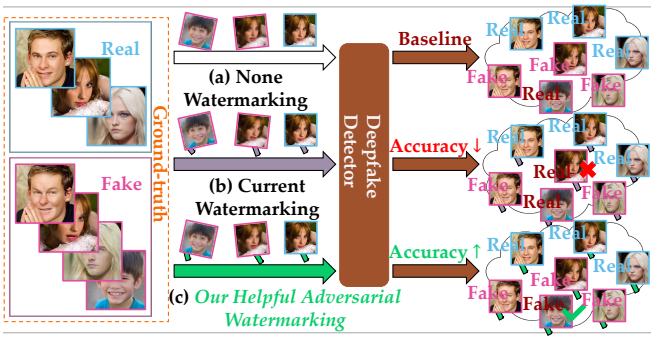

Figure 1: Distinctions between the proposed AdvMark and current watermarking models. (a) Non-watermarked images contributed the baseline of detection performance, where the genuine and forged images may not be easily distinguished. (b) Current watermarking unintentionally degrades the detection performance, since the watermarks are prone to overlap with the forgery signals. (c) Our AdvMark leverages the watermarks to fool Deepfake detectors intentionally, which helps to distinguish between watermarked genuine and forged images without compromising provenance tracking.

Robust watermarking is the prevalent measure for the task of provenance tracking [Zhu *et al.*, 2018; Tancik *et al.*, 2020]. In such a watermarking prototype, subtle watermark signals that identify the provenance are imperceptibly embedded into the host image by a watermark encoder, rendering them almost invisible to the human naked eyes. After that, even if the watermarked image has been subjected to severe distortions, the watermark can still be extracted correctly by a watermark decoder in a blind manner, i.e., without knowledge of the original host image. It is also acknowledged that the watermark embedding can be accomplished during the content generation [Xiong *et al.*, 2023], similar to the encoder implanted into a specific generative model. It should be noted that in this paper, we focus on more general watermarking

*Corresponding author.

methods, which modify the host images and are applicable to arbitrary generative models as well as non-generated images.

In previous studies, proactive watermark injection and passive Deepfake detection were completely independent, without any consideration of their correlation. However, we reveal that in practice, the presence of watermarks leads to more false-negative results when using most passive detectors (see Table 1), which is indeed contrary to the belief in AI responsibility and does a disservice. This can be explained by the fact that current watermarking models were originally devised for genuine images, where the watermarks are prone to overlap with the forgery signals used for detection. One underlying assumption for the watermark effects is that well-trained detectors are asymmetrically tuned to detect patterns that make an image fake [Ojha *et al.*, 2023]. Consequently, anything else without these patterns would be classified as genuine.

To gain more insights into this intriguing phenomenon, we remark that invisible watermarks are analogous to natural adversarial perturbations [Hou *et al.*, 2023]. Both of them are crafted by subtle signals that are not easily perceptible by human eyes; adversarial perturbations are intended to cause misjudgments of the detectors, while watermarks are designed to enable provenance tracking but unintentionally reduce the detection performance. More fundamentally, from the perspective "adversarial examples are features", they can be attributed to non-robust features that are highly predictive for the detectors [Ilyas *et al.*, 2019]. Therefore, in another vein, it is possible for the embedded watermarks to be both recoverable and adversarial at the same time.

To this end, we propose AdvMark, which exploits the adversarial vulnerability of passive detectors for good, making the watermarks adversarial to positively improve the performance of Deepfake detectors. The distinctions between the proposed AdvMark and current watermarking models are observable in Figure 1. Unlike previous harmful adversarial examples and watermarking, our proposed helpful adversarial watermarking deceives the detector into correctly classifying the input image following its ground-truth label. Specifically, in contrast to the original images that were incorrectly predicted, the watermarked images force the detector to report a correct prediction. Meanwhile, the watermarks should not change the detection results of the original correctly predicted images. It is also worth noting that the meaningful watermarks are capable of tracking the image's provenance once extracted, while the meaningless perturbations are not.

Our contributions can be summarized into three-fold:

- We present a harmless proactive forensics solution, AdvMark, which leverages robust watermarking to fool Deepfake detectors for the first time, where the embedded watermarks behave both recoverable and adversarial, thereby achieving the purposes of provenance tracking and detectability enhancement simultaneously.
- To the best of our knowledge, this is the first attempt to formulate the concept of helpful adversarial watermarking, which amends the watermarked images to improve the accuracy of downstream Deepfake detection without tuning the in-the-wild detectors.
- Extensive experiments conducted on well-trained detectors demonstrate the effectiveness of the proposed AdvMark under white- and black-box attacks, on various types of Deepfake, such as face swapping, expression reenactment, attribute editing, and entire synthesis.

2 Related Work

2.1 Deepfake Forensics

Up to now, Deepfake has covered massive types and advanced rapidly, leading to more realistic and convincing face forgeries. To control the dissemination of these, countermeasures are continually developed and can be roughly classified into three categories: passive forensics, proactive defense, and proactive forensics [Wu *et al.*, 2023]. Among them, proactive defense performs adversarial attacks to destroy the creation of Deepfake [Huang *et al.*, 2022]; however, it leaves few forensic clues, as the visually perceptible artifacts are easily perceived and can alert the adversary [Chen *et al.*, 2021].

Passive Forensics. Deep learning-based detectors exploit powerful backbone networks, such as Xception [Rossler *et al.*, 2019] and EfficientNet [Li *et al.*, 2021], and their automatic feature extraction empirically outperforms hand-craft features. CNND [Wang *et al.*, 2020] incorporates appropriate data augmentations during the network training. FFD [Dang *et al.*, 2020] utilizes informative attention maps that indicate suspicious regions to detect the forgery. PatchForensics [Chai *et al.*, 2020] develops the patch-based detector with limited receptive fields to exaggerate local artifacts in patch regions. MultiAtt [Zhao *et al.*, 2021] captures local discriminative features from multiple attentive regions to identify subtle and local differences between genuine and forged images. RFM [Wang and Deng, 2021] erases several sensitive facial regions to guide the detector to allocate more attention to the representative regions. RECCE [Cao *et al.*, 2022] mines common compact representations of genuine faces from the reconstruction perspective. SBI [Shiohara and Yamasaki, 2022] follows the self-supervised paradigm where the more general forgeries can be produced on-the-fly.

Proactive Forensics. To combat Deepfake proactively, FakeTagger [Wang *et al.*, 2021] is derived from robust watermarking, where the embedded watermarks can survive both before and after Deepfake, enabling the tracking of the provenance of watermarked images. FaceSigns [Neekhara *et al.*, 2022] introduces a semi-fragile watermarking framework, and its proactive detection is realized through verifying the extracted watermarks. SepMark [Wu *et al.*, 2023] enables the embedded watermark to be extracted at different levels of robustness, achieving the purposes of provenance tracking and proactive detection simultaneously. Likewise, BiFPro [Liu *et al.*, 2023] extends watermarking into diverse forensic scenarios where the watermark manifests either fragility or robustness. The embedded watermarks can be identity-related messages [Zhao *et al.*, 2023b; Wang *et al.*, 2023; Guan *et al.*, 2023]. Other than deep watermarking, Source-ID-Tracker [Lin *et al.*, 2022] employs steganography to hide the original images within their forged versions. PIMD [Asnani *et al.*, 2022] and MaLP [Asnani *et al.*, 2023] add the learned templates to conduct proactive detection and location, respectively. Moreover, AFP [Yu *et al.*, 2021] and Faketracer

[Sun *et al.*, 2022a] poison the training data, resulting in watermarked generative models.

2.2 Adversarial Attacks

Seminal work [Szegedy *et al.*, 2014] discloses the vulnerable nature of deep neural networks to adversarial examples. Transferability is an intriguing property of adversarial examples; deliberately perturbed inputs generated for the surrogate model can mislead other victim models' predictions. Adversarial attacks can be categorized as white-box and black-box, depending on whether the target model can be accessed (e.g., architecture and parameters). Moreover, untargeted attacks aim to cause the model to misclassify inputs regardless of the specific category. Accordingly, targeted attacks aim to cause the model to misclassify inputs into another specific category. Notably, the generative attacks [Poursaeed *et al.*, 2018; Xiao *et al.*, 2018] leverage a trainable generator to directly generate desired perturbations, which are ingeniously similar to current watermarking models and require only a single forward pass in the inference stage, as opposed to instance-specific iterative optimization attacks. For more details on this avenue, the review [Zhao *et al.*, 2023c] is recommended.

3 Motivation & Insight

Motivation. The previous proactive defense method [Wang *et al.*, 2022b] takes the downstream task of passive forensics into consideration, where the attacked unrealistic Deepfake should be effortlessly recognized by the detectors. It is noteworthy that the proactive defense methods [Zhu *et al.*, 2023; Zhang *et al.*, 2024b] also consider proactive forensics, providing the adversarial perturbations with the forensic clue that is capable of provenance tracking. However, the research regarding the correlation between proactive forensics and passive forensics remains substantially unfilled. To study how the watermarks impact Deepfake detectors, we report the detection results of the images watermarked by MBRS [Jia *et al.*, 2021], FaceSigns, and SepMark, which represent robust, semi-fragile, and multipurpose watermarking, respectively. Table 1 shows that the detectors have a clear tendency to predict the watermarked forged images as genuine. To rectify this, a harmless proactive forensics solution is urgently needed, which should concurrently take the downstream Deepfake detectors into consideration, where the watermarked images should be more easily distinguished by the Deepfake detectors, relative to non-watermarked images.

Insight. Although the term "adversarial" leaves an indelible impression of its malicious functionality, adversarial training for benign purposes can effectively boost model robustness. What's more, along with the belief in "adversarial for good" [Al-Maliki *et al.*, 2024], if harnessed in the right manner, the adversarial nature can be utilized to improve image recognition models [Xie *et al.*, 2020], amend the accuracy level of neural models [Yu *et al.*, 2023], boost object detection performance [Sun *et al.*, 2022b], protect watermarks against removal [Liu *et al.*, 2022], prevent automatic painting imitation [Liang *et al.*, 2023] and Deepfake generation [Wang *et al.*, 2022a]. In a similar vein, we delve into robust watermarking to exploit the adversarial vulnerability of Deepfake detectors for good. Note that this paper is not focusing on developing a new robust watermarking model or a new Deepfake detector. Instead, we propose a plug-and-play targeted attack procedure for fine-tuning any robust watermarking to help improve the accuracy of downstream Deepfake detection without tuning the detectors (see Figure 2). Concretely, during our adversarial fine-tuning procedure, only the parameters of watermarking models are updated, and Deepfake detectors keep unchanged. Fine-tuning robust watermarking into adversarial watermarking involves several challenges and key factors. First, it's crucial that the detector attack exhibits efficacy in both white- and black-box scenarios, with adversarial transferability occupying a pivotal position. Secondly, the watermark extraction should still be conducted successfully to enable provenance tracking. Lastly, the visual quality of the watermarked images should remain pleasing.

		Xception	EfficientNet	CNND
Clean	Real ACC	98.19	99.11	99.96
	Fake ACC	20.82	52.73	27.87
JPEG	Real ACC	84.49	1.13	99.89
	Fake ACC	32.15	99.89	18.06
Gaussian Noise	Real ACC	99.93	25.07	100.0
	Fake ACC	0.00	82.61	0.32
MBRS [Jia *et al.*, 2021]	Real ACC	98.73	98.83	99.96
	Fake ACC	17.53	45.29	23.41
FaceSigns [Neekhara *et al.*, 2022]	Real ACC	98.62	98.83	99.82
	Fake ACC	10.91	38.60	23.09
SepMark [Wu *et al.*, 2023]	Real ACC	98.44	99.47	99.96
	Fake ACC	15.30	28.26	24.11

Table 1: Accuracy of well-trained Deepfake detectors tested on non-watermarked/JPEG-compressed/Gaussian noisy/watermarked images in detecting separate real and fake subsets. We have the following observations: i) the detectors predict almost all the genuine images with high accuracy, regardless of whether they are watermarked or not, but struggle with diverse types of forged images; ii) the watermarks distort the images in a counter-intuitive fashion, which is actually different from JPEG and Gaussian noise; and iii) the watermarked forged images are more likely to be predicted as real by the detectors, compared to the non-watermarked forged counterparts. The experimental setup here is consistent with Section 5.

4 Methodology

4.1 Problem Formulation

Adversarial Perturbations Harm Detectors. Let x denote the clean host image, and y denote its ground-truth label. We use $\hat{x}$ to represent the adversarial image, i.e., $\hat{x} = x + \eta$, where η is the imperceptible perturbation with the L_p-norm constraint $\|\eta\|_p \leq \epsilon,\ p \in \{0, 2, \infty\}$. Suppose there is a perturbation generator $\mathcal{P}(\cdot)$ generating the perturbations directly, i.e., $\hat{x} = x + \mathcal{P}(x)$, and a Deepfake detector $\mathcal{D}(\cdot)$ predicting the label of the input. We recall the vanilla adversarial attack, where the objective is to mislead the detector into making an incorrect prediction by

$$\max_{\mathcal{P}} \mathbb{E}_{(x,y)}\ \mathcal{F}(\mathcal{D}(x + \mathcal{P}(x)), y), \tag{1}$$

where $\mathcal{F}$ denotes the commonly used cross-entropy loss or binary cross-entropy loss for the task of Deepfake detection. It should be noted that the perturbations generated by $\mathcal{P}(\cdot)$ are typically constrained by a small L_∞-norm budget, to maintain the lower bound of visual quality but may not align well with human perception, with respect to perturbed images.

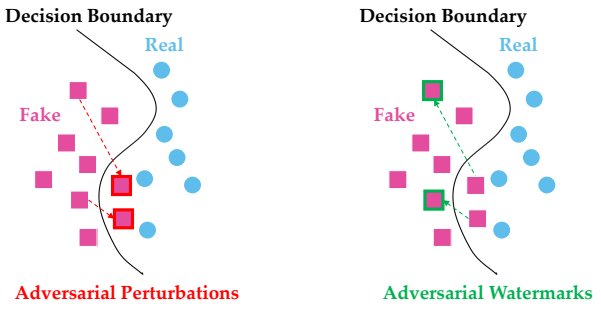

Figure 2: The sketch of adversarial perturbations vs. adversarial watermarks. Left: The objective of adversarial perturbations is to make correctly predicted inputs result in wrong detection outcomes. Right: The objective of adversarial watermarks is to make original incorrectly predicted inputs yield correct detection outcomes.

Adversarial Watermarks Help Detectors. Given a watermark encoder $En(\cdot)$ with the input of the host image x and watermark w, we can obtain the watermarked image x_w, i.e., $x_w = En(x, w)$. A corresponding watermark decoder $De(\cdot)$ should be able to extract the watermark w exactly from the image x_w. Nevertheless, considering that the watermarked image is sometimes delivered and distributed through the dirty channel, it is proposed to introduce a noise layer $\mathcal{N}(\cdot)$ to distort the image x_w with diverse data augmentations, where the distorted image $\widetilde{x_w} = \mathcal{N}(x_w)$. In this way, the robust decoder can extract an approximate watermark from the image $\widetilde{x_w}$, i.e., $\widetilde{w} = De(\widetilde{x_w})$, meaning $\widetilde{w} \approx w$. Formally, the objective of our adversarial watermarking, which helps the detector classify watermarked images, can be formulated as

$$\min_{En,De} \mathbb{E}_{(x,y,w)} \left[\mathcal{F}(\mathcal{D}(En(x,w)), y) + \mathcal{G}(En(x,w), x) + \mathcal{H}(De(\mathcal{N}(En(x,w))), w)\right], \tag{2}$$

where $\mathcal{G}$ denotes the loss function used for image similarity measures (e.g., mean-squared error loss and LPIPS loss [Zhang *et al.*, 2018]), and $\mathcal{H}$ represents the mean-squared error loss or binary cross-entropy loss, which usually characterizes the watermark extraction as either a regression or a classification problem, respectively.

4.2 AdvMark Framework

As illustrated in Figure 3, the pipeline of our proposed AdvMark consists of five components: *Watermark Encoder*, *Noise Layer*, *Watermark Decoder*, *Adversary Discriminator* and downstream *Deepfake Detector*. Specifically, we showcase the functionalities of each component as follows:

1) The encoder En receives a batch of the host image $x \in \mathbb{R}^{B\times 3\times H\times W}$ (which belongs to either genuine or forged, labeled by $y \in \{0,1\}^{B\times 1}$), and random watermark bits $w \in \{0,1\}^{B\times L}$ as input. It produces the watermarked image x_w, which has intriguing adversarial properties for helping the downstream Deepfake detectors.
2) The noise layer $\mathcal{N}$ augments the watermarked image x_w with various simulated or real distortions, resulting in the distorted image $\widetilde{x_w}$. It is parameterless but differentiable, which connects the encoder En and decoder De to facilitate end-to-end robust training.

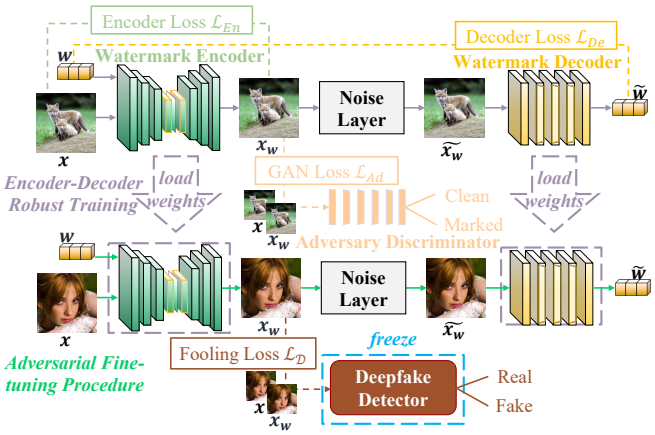

Figure 3: Overview of our proposed AdvMark. The training process consists of two stages. In Stage I, the encoder and decoder are jointly trained end-to-end, obtaining the pre-trained encoder and decoder that serve as robust watermarking. In Stage II, the encoder and decoder are fine-tuned end-to-end by fooling a surrogate Deepfake detector, aiming at transforming robust watermarking into adversarial watermarking. During inference, only the final watermark encoder and decoder will be adopted.

3) The decoder De extracts the watermark $\widetilde{w}$ from the distorted image $\widetilde{x_w}$, where $\widetilde{w} \approx w$, to reliably track the provenance of watermarked image x_w. Note that it also participates in updating the encoder En to generate the image that is more conducive to watermark extraction.
4) The adversary discriminator Ad attempts to distinguish between the host image x and the watermarked image x_w. Conversely, the encoder En should mislead the discriminator so that Ad cannot distinguish x_w from x, to acquire better visual quality of the watermarked image.
5) The surrogate detector $\mathcal{D}$ classifies the watermarked image x_w as genuine or forged. In the case of $\mathcal{D}(x) \neq y$, the watermarked image generated by the encoder En makes sense when $\mathcal{D}(x_w) = y$, reflecting the enhanced forensic detectability. This watermarked image is even easier to be detected by other downstream detectors.

Below we will provide a detailed description of the pre-training stage of robust watermarking, the fine-tuning stage of adversarial watermarking, and the inference stage of final watermark encoder and decoder in turn.

Encoder-Decoder Robust Training. For the watermark encoder En, its watermarked image x_w should be visually similar to the original host image x:

$$\mathcal{L}_{En} = L_2(x, x_w) = L_2(x, En(\theta; x, w)), \tag{3}$$

where θ denotes the trainable parameters of the encoder.

For the watermark decoder De, its extracted watermark $\widetilde{w}$ should be identical to the original embedded watermark w, from the distorted image $\widetilde{x_w}$ augmented by noise layer $\mathcal{N}$:

$$\mathcal{L}_{De} = L_2(w, \widetilde{w}) = L_2(w, De(\phi; \widetilde{x_w})), \tag{4}$$

where

$$\widetilde{x_w} = \mathcal{N}(x_w) = \mathcal{N}(En(\theta; x, w)), \tag{5}$$

and ϕ represents the trainable parameters of the decoder.

For the adversary discriminator Ad, there are several loss variants for stabilizing the GAN training [Jolicoeur-Martineau, 2019], and for ease of presentation, here we describe the standard GAN loss [Goodfellow *et al.*, 2014]:

$$\mathcal{L}_{Adv} = \log(1 - Ad(\gamma; En(x, w))) + \log(Ad(\gamma; x)), \quad (6)$$

where γ indicates the trainable parameters of the discriminator. Note that the discriminator is trained alternately with the encoder-decoder, where the encoder En is also updated by

$$\mathcal{L}_{Ad} = \log(Ad(x_w)) = \log(Ad(En(\theta; x, w))). \quad (7)$$

To sum up, the total loss for Stage I can be formulated by

$$\mathcal{L}_I = \lambda_1 \mathcal{L}_{En} + \lambda_2 \mathcal{L}_{De} + \lambda_3 \mathcal{L}_{Ad}, \quad (8)$$

where λ_1, λ_2, λ_3 are the weights for respective loss terms. After training, we get the pre-trained encoder En_I and decoder De_I. We can also freely adopt the released models[1,2] as the pre-trained encoder and decoder for this stage. More implementation details can be found in Section 5.2.

Adversarial Fine-tuning Procedure. The advent of highly realistic generated content can easily deceive human eyes. Manually examining a large volume of images through observation is extremely expensive, even when the defects are obvious. Therefore, it is preferable to develop automatic Deepfake detectors on the machine end. However, with the proliferation of generated images, merely verifying their authenticity seems insufficient without understanding their provenance, since it's difficult to differentiate between images created for malicious intents and those created for neutral or positive purposes. Building upon the watermarking at Stage I, a responsible individual or social network can embed the provenance evidence into the published images using his/her watermark encoder En_I. Unfortunately, the proactive injection will harm the passive detectors, which are more prevalent and widely deployed in the wild than the solely watermark decoder De_I. This is indeed contrary to the belief in AI responsibility and does a disservice. In light of the above, we propose a plug-and-play targeted attack procedure that fine-tunes robust watermarking into adversarial watermarking, aiming to help improve the accuracy of downstream Deepfake detection by deliberately fooling the passive detectors (i.e., crossing the decision boundary; see Figure 2).

To achieve the fooling objective, we freeze a surrogate detector $\mathcal{D}$ and force the detector to predict the correct label y with respect to the watermarked image x_w by updating En_I:

$$\mathcal{L}_{\mathcal{D}} = \mathcal{F}(\mathcal{D}(x_w), y) = \mathcal{F}(\mathcal{D}(En_I(\theta; x, w)), y), \quad (9)$$

where $\mathcal{F}$ denotes the loss function (e.g., binary cross-entropy loss) used to train the original detector $\mathcal{D}$.

To summarize, the total loss for Stage II is formulated by

$$\mathcal{L}_{II} = \lambda_1 \mathcal{L}_{En} + \lambda_2 \mathcal{L}_{De} + \lambda_3 \mathcal{L}_{Ad} + \lambda_4 \mathcal{L}_{\mathcal{D}}, \quad (10)$$

where λ_4 is the weight for the fooling loss term. After fine-tuning, we get the final encoder En_{II} and decoder De_{II}. Detecting the watermarked images amended by En_{II} will help improve detection accuracy without tuning the detectors.

[1]https://github.com/jzyustc/MBRS

[2]https://github.com/sh1newu/SepMark

Model Inference. In the inference process, only the well-trained watermark encoder En_{II} and decoder De_{II} are adopted. Consequently, depending on our adversarial watermarks, we can categorize the harmless proactive forensics into the following cases.

Case 1: If $\widetilde{w} \not\approx w$, the suspicious image is either not watermarked by the encoder En_{II} at all or has been extremely altered by significant distortions, reflecting that it is impossible to track its provenance by the decoder De_{II}.

Case 2: If $\widetilde{w} \approx w$, the image has been watermarked by the encoder En_{II}, and we can extract the watermark $\widetilde{w}$ to serve as evidence of the image's provenance, and effortlessly determine whether it is genuine or forged by the detector $\mathcal{D}$, which we refer to as enhanced forensic detectability.

Case 3: Even in a more challenging setting where the detector $\mathcal{D}'$ was unseen during the training process, the watermarked image x_w is also more easily distinguished by $\mathcal{D}'$, which is known as adversarial transferability.

5 Experiments

5.1 Dataset Preparation

We collect the real faces sourced from CelebA-HQ [Karras *et al.*, 2018] and resize them to the resolution of 256×256. These real faces are then manipulated by recent Deepfake generative models: SimSwap [Chen *et al.*, 2020] for face swapping, FOMM [Siarohin *et al.*, 2019] for expression reenactment, and StarGAN [Choi *et al.*, 2018] for attribute editing. We further utilize the entire synthesized faces provided by StyleGAN [Karras *et al.*, 2019], which are also resized to 256×256. These four fake categories are evenly sampled to balance the numbers of real and fake faces. More specifically, there are equal numbers of faces in real and fake subsets, and we divide them into training, validation, and testing, respectively, referencing the official split $24183/2993/2824$.

5.2 Implementation Details.

As the proposed work is not focusing on developing a new robust watermarking model, we directly adopt MBRS and the robust branch of SepMark as the pre-trained encoder and decoder in Stage I, and also as our baselines. To show that the performance gain is due to our adversarial fine-tuning procedure rather than training for more iterations, we establish additional baselines where the two watermarking models undergo a vanilla fine-tuning procedure (without fooling loss) on the dataset. Moreover, we utilize nine well-trained Deepfake detectors, as described in Section 2.1, to validate the capability of forensic detectability and adversarial transferability. For the hyper-parameter settings of MBRS and SepMark, we strictly follow their original implementations. For example, besides the difference in the length of the watermark bits (256-bit for MBRS and 128-bit for SepMark), the noise layers they use are also inconsistent. To be specific, MBRS includes *Identity*, *JPEG*, and *simulated JPEG*, while SepMark contains all the noises listed in Table 3. Therefore, we will compare our AdvMark with the respective baselines for each to mitigate the model bias introduced by different backbones. Lastly, the whole fine-tuning lasted for 10 epochs with a batch size of 8, and we set the weight of the fooling loss λ_4 to 0.1.

	Xception	EfficientNet	CNND	FFD	PatchForensics	MultiAtt	RFM	RECCE	SBI	Average
Clean	98.19/20.82	99.11/52.73	99.96/27.87	97.17/59.67	99.40/33.43	85.23/20.36	39.41/82.33	54.36/60.38	87.57/30.06	84.49/43.07
JPEG	84.49/32.15	1.13/99.89	99.89/18.06	99.96/0.11	100.0/0.00	91.25/13.39	98.87/0.21	92.92/15.16	90.93/17.17	84.38/21.79
Gaussian Noise	99.93/0.00	25.07/82.61	100.0/0.32	96.53/5.45	100.0/0.00	77.58/20.54	85.98/5.67	29.99/86.54	99.96/0.11	79.45/22.36
MBRS	98.73/17.53	98.83/45.29	99.96/23.41	94.33/54.21	99.36/30.38	84.77/20.01	42.92/79.78	69.19/44.97	89.34/26.17	86.38/37.97
+ Vanilla Fine-tuning	98.41/18.41	97.77/52.83	99.93/19.12	97.06/41.04	99.65/31.94	86.23/19.37	43.73/79.14	63.99/49.50	87.89/27.90	86.07/37.69
+ AdvMark (Xception)	99.82/99.82*	99.04/95.04	99.96/5.67	96.49/1.88	98.26/69.26	87.68/0.92	78.15/24.68	74.79/82.75	95.08/5.88	92.14/42.88
+ AdvMark (Efficient.)	99.08/15.58	100.0/99.89*	99.96/21.00	98.37/22.06	84.77/54.64	88.07/18.56	63.99/77.87	79.04/38.56	92.81/26.13	89.57/41.59
+ AdvMark (CNND)	98.97/15.90	41.57/51.13	99.68/99.47*	97.59/49.86	86.97/83.14	89.09/25.28	96.14/84.24	86.69/9.67	94.05/10.30	87.86/47.67
+ AdvMark (FFD)	99.65/10.34	76.06/30.84	99.93/13.63	86.19/94.19*	47.27/82.37	83.04/23.23	65.93/75.99	71.53/33.60	85.91/34.70	79.50/44.32
+ AdvMark (PatchFor.)	98.94/8.53	94.79/84.45	99.96/7.19	98.41/24.04	100.0/99.96*	86.61/13.88	99.72/25.32	77.83/30.67	89.73/18.63	94.00/34.74
+ AdvMark (MultiAtt)	99.15/35.87	96.74/94.83	99.96/13.03	98.48/40.51	98.12/64.45	100.0/100.0*	91.68/94.44	99.65/80.63	99.01/25.53	98.09/61.03
+ AdvMark (RFM)	99.08/15.30	92.25/72.10	99.96/23.90	96.42/48.90	96.67/60.62	88.00/18.02	100.0/100.0*	70.61/42.07	91.43/25.99	92.71/45.21
+ AdvMark (RECCE)	99.72/18.20	35.30/94.55	99.96/19.09	99.79/34.60	100.0/57.01	95.75/19.26	52.83/70.93	100.0/100.0*	98.55/11.01	86.88/47.18
+ AdvMark (SBI)	99.58/41.75	99.26/89.31	99.96/20.40	99.01/22.45	96.74/34.60	96.18/46.57	90.79/80.88	95.89/88.17	100.0/99.43*	97.49/58.17
+ AdvMark (Ensemble)	99.89/99.08*	88.99/96.42	99.96/21.21	83.32/28.58	99.82/68.87	99.96/99.72*	100.0/99.93*	91.78/98.51	98.58/63.88	95.81/75.13
SepMark	98.44/15.30	99.47/28.26	99.96/24.11	94.62/59.45	99.15/37.50	87.75/18.02	36.30/81.06	59.81/51.70	89.13/22.45	84.96/37.54
+ Vanilla Fine-tuning	98.09/19.51	98.37/44.16	99.96/25.11	92.71/61.05	98.34/39.87	86.54/17.46	34.81/82.65	62.54/50.46	86.37/26.35	84.19/40.74
+ AdvMark (Xception)	99.82/99.68*	98.76/70.08	99.96/29.39	92.42/66.43	99.40/43.66	89.73/64.48	29.53/82.54	73.02/95.04	93.41/87.46	86.23/70.97
+ AdvMark (Efficient.)	98.55/23.09	99.96/99.82*	99.96/26.81	92.81/62.61	99.15/36.05	87.75/24.08	36.83/81.94	68.31/66.47	89.59/40.47	85.88/51.26
+ AdvMark (CNND)	99.29/21.10	98.94/52.62	99.89/97.84*	90.01/62.64	97.73/47.42	85.30/16.82	38.53/83.00	59.42/57.47	93.09/31.83	84.69/52.30
+ AdvMark (FFD)	98.76/17.99	99.33/45.89	99.96/25.92	98.90/95.64*	99.68/39.24	86.30/20.33	37.71/83.82	62.71/58.11	92.28/25.81	86.18/45.86
+ AdvMark (PatchFor.)	98.69/18.70	99.22/37.96	99.96/23.94	96.00/86.93	99.96/99.82*	88.31/16.11	38.63/88.81	69.02/46.03	91.82/22.38	86.85/48.96
+ AdvMark (MultiAtt)	99.33/46.81	97.70/83.82	99.89/23.80	92.92/63.07	95.72/54.43	99.86/99.93*	33.68/86.69	95.68/97.42	95.36/70.29	90.02/69.58
+ AdvMark (RFM)	98.26/18.52	99.11/56.34	99.93/22.66	94.44/68.56	99.65/43.31	86.23/21.85	99.15/100.0*	59.42/57.22	85.38/30.21	91.29/46.52
+ AdvMark (RECCE)	99.43/27.37	98.76/60.30	99.96/27.02	92.35/67.28	98.37/39.52	97.63/55.13	39.02/83.32	99.96/99.96*	93.84/50.11	91.04/56.67
+ AdvMark (SBI)	98.83/28.36	99.01/56.41	99.96/24.47	89.34/56.34	98.94/37.36	90.86/32.51	34.07/83.11	71.78/75.53	99.58/98.83*	86.93/54.77
+ AdvMark (Ensemble)	99.40/97.91*	98.87/87.36	99.96/30.49	93.94/75.18	99.65/40.08	99.22/99.47*	99.04/99.86*	92.56/98.12	93.20/85.87	97.32/79.37

Table 2: Detection accuracy (Real/Fake ACC ↑) under white & black-box attacks. " * " indicates seen detector during training.

5.3 Detector Attack

The benign functionality of adversarial watermarking is confirmed in both white- and black-box scenarios. The evaluation metric here is the accuracy (ACC) of the detector $\mathcal{D}$:

$$ACC(\mathcal{D}) = \frac{1}{B}\sum_{i=1}^{B} |\mathcal{D}(x^{i\times 3\times H\times W}) - y^{i\times 1}| \times 100\%, \quad (11)$$

where

$$\mathcal{D}(x) = \begin{cases} 0 & \text{if } x \text{ is predicted as real,} \\ 1 & \text{if } x \text{ is predicted as fake,} \end{cases} \quad (12)$$

and $y \in \{0,1\}^{B\times 1}$ means the ground-truth label, $|\cdot|$ denotes the absolute value. For a comprehensive evaluation, we report the Real/Fake ACC on the separate real and fake subsets. The higher the value, the better the detection performance.

White-box Attack. In the white-box scenario, we evaluate the "training accuracy" with the detector seen during training. When the watermark encoder-decoder and Deepfake detector are in the same camp, i.e., the detector is already known by the watermarking developer, the surrogate detector used can be consistent with the downstream detector. By observing Table 2, we note that the white-box detector without any tuning can get significant performance gain in detecting the images watermarked by AdvMark. The baselines MBRS and SepMark are similar to the image processing operations, e.g., JPEG compression and Gaussian noise, which are harmful to the detector, where they distort the host image in different fashions. The fine-tuned baselines also have inferior detection performance compared to the clean host images without watermarking. By contrast, our helpful AdvMark turns the watermark from an enemy into a friend, ensuring nearly 100% accuracy for the detector in the white-box setting. This is also the case when several detectors, e.g., Xception, MultiAtt, and RFM, are included for the adversarial fine-tuning.

Black-box Attack. We further evaluate the "testing accuracy" with the detector unseen during training, in the black-box scenario. Table 2 shows that compared to the clean host images, the watermarked images using AdvMark are more easily distinguished by other unseen detectors, thanks to the transferability of adversarial watermarks. For example, using MultiAtt or SBI as the surrogate detector, the resulting detection performance with AdvMark is higher than that without watermarking, on average. We notice that AdvMark is inferior to the baselines on a few unseen detectors, which may be due to the different decision logic shared by the detectors. E.g., most detectors mainly identify distinct fake patterns in the images, while the exception RECCE seeks to discriminate what is real. Since AdvMark performs quite well in the white-box setting, we speculate that it has the potential to overfit to the seen detector, but on some unseen detectors it may have ruined the detection. Suggested by ensemble attacks [Poursaeed *et al.*, 2018], we can attack an ensemble of detectors, which is more conducive in the real world. By simultaneously attacking Xception, MultiAtt, and RFM, in the black-box setting we obtain an overall improved detection performance, which is indeed better than attacking only one detector.

5.4 Watermark Extraction & Visual Quality

Since our AdvMark focuses on improving the forensic detectability of watermarked images without compromising provenance tracking, we expect as few performance degradations in Bit Error Rate (BER) as possible. Suppose that the embedded watermark $w \in \{0,1\}^{B\times L}$ and the extracted watermark $\widetilde{w} \in \{0,1\}^{B\times L}$, formally,

$$BER(w,\widetilde{w}) = \frac{1}{B}\times\frac{1}{L}\times\sum_{i=1}^{B}\sum_{j=1}^{L}|w^{i\times j} - \widetilde{w}^{i\times j}| \times 100\%. \quad (13)$$

	Identity	JPEG	Resize	GB	MB	Brightness	Contrast	Saturation	Hue	Dropout	SP	GN	Average	PSNR (dB)	SSIM
MBRS	0.0001	0.253	1.764	3.528	2.290	1.002	1.143	0.001	0.001	0.048	31.87	13.10	4.583	44.31	0.972
+ Vanilla Fine-tuning	0.000	0.160	2.615	0.204	0.196	1.035	0.984	0.001	0.001	0.037	37.34	13.06	4.636	43.98	0.975
+ AdvMark (Xception)	0.000	0.909	0.058	3.246	7.115	1.021	0.672	0.001	0.280	0.153	9.293	6.736	2.457	38.72	0.909
+ AdvMark (Efficient.)	0.000	0.689	0.004	0.538	0.370	1.100	0.868	0.001	0.031	0.013	14.26	13.30	2.598	41.88	0.955
+ AdvMark (CNND)	0.0001	1.469	0.358	14.67	19.21	0.772	0.227	0.001	0.425	0.246	15.48	2.251	4.592	34.00	0.848
+ AdvMark (FFD)	0.001	0.349	0.782	1.643	2.675	0.847	0.489	0.001	0.002	0.029	21.48	0.362	2.388	34.67	0.894
+ AdvMark (PatchFor.)	0.000	0.455	4.961	5.675	13.43	0.998	0.465	0.000	0.000	0.007	25.74	1.262	4.416	36.70	0.912
+ AdvMark (MultiAtt)	0.000	0.169	0.058	0.652	0.711	1.043	0.865	0.000	0.040	0.007	16.44	5.533	2.127	36.20	0.876
+ AdvMark (RFM)	0.000	0.743	0.699	1.728	1.813	1.065	0.958	0.001	0.002	0.049	28.70	9.678	3.786	43.14	0.967
+ AdvMark (RECCE)	0.000	1.586	0.011	0.188	0.151	1.121	1.197	0.003	0.231	0.014	8.891	15.94	2.444	39.10	0.908
+ AdvMark (SBI)	0.000	0.974	0.025	0.561	0.395	1.169	0.984	0.001	0.156	0.051	12.26	12.47	2.421	38.84	0.926
+ AdvMark (Ensemble)	0.000	1.830	1.640	3.632	3.850	1.014	1.003	0.002	1.473	0.019	19.48	7.792	3.478	37.38	0.916
SepMark	0.005	0.006	0.0001	0.0001	0.001	0.011	0.004	0.006	0.008	0.112	0.0004	0.066	0.018	38.52	0.930
+ Vanilla Fine-tuning	0.000	0.004	0.000	0.000	0.000	0.003	0.000	0.000	0.000	0.000	0.000	0.088	0.008	40.66	0.948
+ AdvMark (Xception)	0.000	0.027	0.0001	0.000	0.000	0.001	0.000	0.000	0.000	0.0001	0.0001	0.111	0.012	37.97	0.924
+ AdvMark (Efficient.)	0.000	0.274	0.001	0.0003	0.0001	0.006	0.001	0.000	0.000	0.003	0.005	1.128	0.118	42.13	0.961
+ AdvMark (CNND)	0.000	0.576	0.003	0.001	0.0004	0.005	0.001	0.000	0.000	0.001	0.001	1.341	0.161	39.63	0.945
+ AdvMark (FFD)	0.000	1.891	0.016	0.007	0.011	0.010	0.004	0.000	0.0001	0.011	0.014	3.432	0.450	44.49	0.977
+ AdvMark (PatchFor.)	0.000	0.119	0.001	0.000	0.000	0.003	0.001	0.000	0.000	0.001	0.001	0.572	0.058	41.57	0.955
+ AdvMark (MultiAtt)	0.000	0.007	0.000	0.000	0.000	0.002	0.000	0.000	0.000	0.0001	0.0001	0.112	0.010	38.46	0.925
+ AdvMark (RFM)	0.000	0.288	0.001	0.0003	0.0001	0.003	0.0004	0.000	0.000	0.000	0.0003	1.008	0.108	42.12	0.961
+ AdvMark (RECCE)	0.000	0.122	0.0003	0.000	0.000	0.002	0.000	0.000	0.000	0.001	0.0003	0.551	0.056	39.87	0.947
+ AdvMark (SBI)	0.000	0.156	0.001	0.000	0.000	0.004	0.001	0.000	0.000	0.0004	0.001	0.700	0.072	40.12	0.949
+ AdvMark (Ensemble)	0.000	0.054	0.0001	0.0001	0.000	0.003	0.000	0.000	0.000	0.0001	0.0001	0.287	0.029	38.18	0.928

Table 3: Extraction error rate (BER ↓) & PSNR (↑) and SSIM (↑) of watermarked images. "0.000" indicates error-free extraction. Gaussian Blur, Median Blur, Salt Pepper, and Gaussian Noise are abbreviated as GB, MB, SP, and GN, respectively.

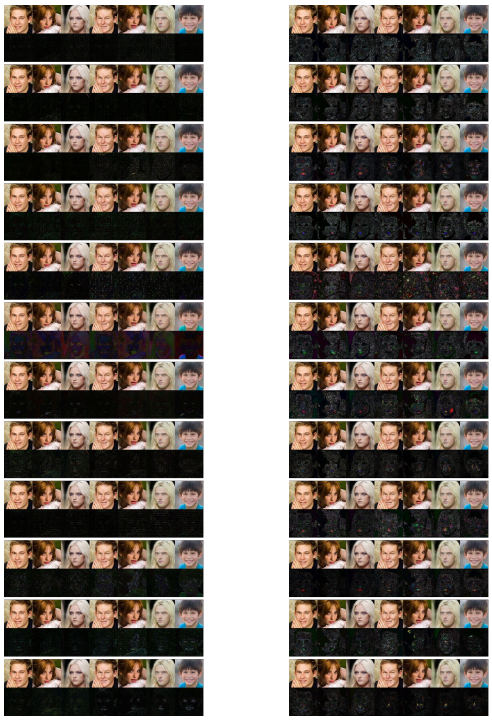

(a) MBRS (b) SepMark

Figure 4: Visualizations on watermarked images and normalized residuals. From top to bottom, refer to the default order in Table 3.

A lower BER indicates stronger robustness in watermark extraction. From Table 3, we can see that the BER of AdvMark is comparable to the baselines, and the performance gaps are almost negligible, regardless of the surrogate detector used. Interestingly, the adversarially fine-tuned MBRS enhances the robustness against unseen distortions, e.g., salt pepper and Gaussian noise, which is likely due to the redundancy of embedded adversarial watermarks. The robustness resists against distortion attacks may depend on the utilized watermarking backbone; it shall be even greater when using a more advanced watermarking backbone.

Although AdvMark accomplishes both provenance tracking and detectability enhancement, we have to admit that these benefits come at the cost of visual quality to a certain extent. As seen in Table 3, the watermarked images using AdvMark exhibit distinct PSNR and SSIM values that can vary for different surrogate detectors. Despite these trade-offs, the subjective visual quality should still be pleasurable. Figure 4 visualizes the watermarked images and their min-max normalized residual signals relative to clean host images. By observation, we speculate that the rationale behind the watermark residuals may be attributed to the real or fake patterns associated with the decision logic of the detector. While the watermarked images have distinct residual patterns, the subjective visual quality still aligns well with human perception.

6 Conclusion

In this work, we make the first attempt to bridge proactive forensics and passive forensics, the two previously uncorrelated studies, and propose the concept of helpful adversarial watermarking, reflecting the belief in "adversarial for good". Without training the watermarking model from scratch, AdvMark can serve as a plug-and-play procedure, seamlessly integrating with existing watermarking. By fine-tuning robust watermarking into adversarial watermarking, we do not harm the performance of passive detectors while fulfilling proactive forensics, achieving harmless provenance tracking and concurrently enhancing forensic detectability. We also investigate the transferability of adversarial watermarks, allowing AdvMark to generalize the watermarking to unseen Deepfake detectors, further validating its effectiveness in the wild. In our future work, we plan to conduct more analyses of the watermark effects on other downstream tasks, such as tamper localization [Zhang *et al.*, 2024a].

Acknowledgments

This work is supported by National Natural Science Foundation of China (Grant Nos. U22A2030, U20A20174), National Key R&D Program of China (Grant No. 2022YFB3103500), Hunan Provincial Funds for Distinguished Young Scholars (Grant No. 2024JJ2025). Supplementary material, including more details and experiments of our work, can be found in the supplement at https://github.com/sh1newu/AdvMark.

References

[Al-Maliki *et al.*, 2024] Shawqi Al-Maliki, Adnan Qayyum, Hassan Ali, Mohamed Abdallah, Junaid Qadir, Dinh Thai Hoang, Dusit Niyato, and Ala Al-Fuqaha. Adversarial machine learning for social good: Reframing the adversary as an ally. *IEEE TAI*, 2024.

[Asnani *et al.*, 2022] Vishal Asnani, Xi Yin, Tal Hassner, Sijia Liu, and Xiaoming Liu. Proactive image manipulation detection. In *CVPR*, 2022.

[Asnani *et al.*, 2023] Vishal Asnani, Xi Yin, Tal Hassner, and Xiaoming Liu. Malp: Manipulation localization using a proactive scheme. In *CVPR*, 2023.

[Bui *et al.*, 2023] Tu Bui, Shruti Agarwal, Ning Yu, and John Collomosse. Rosteals: Robust steganography using autoencoder latent space. In *CVPRW*, 2023.

[C2PA, 2021] C2PA. Coalition for content provenance and authenticity. https://c2pa.org/, 2021. Accessed: 2023-07.

[Cao *et al.*, 2022] Junyi Cao, Chao Ma, Taiping Yao, Shen Chen, Shouhong Ding, and Xiaokang Yang. End-to-end reconstruction-classification learning for face forgery detection. In *CVPR*, 2022.

[Chai *et al.*, 2020] Lucy Chai, David Bau, Ser-Nam Lim, and Phillip Isola. What makes fake images detectable? understanding properties that generalize. In *ECCV*, 2020.

[Chen *et al.*, 2020] Renwang Chen, Xuanhong Chen, Bingbing Ni, and Yanhao Ge. Simswap: An efficient framework for high fidelity face swapping. In *ACM MM*, 2020.

[Chen *et al.*, 2021] Zhikai Chen, Lingxi Xie, Shanmin Pang, Yong He, and Bo Zhang. Magdr: Mask-guided detection and reconstruction for defending deepfakes. In *CVPR*, 2021.

[Choi *et al.*, 2018] Yunjey Choi, Minje Choi, Munyoung Kim, Jung-Woo Ha, Sunghun Kim, and Jaegul Choo. Stargan: Unified generative adversarial networks for multi-domain image-to-image translation. In *CVPR*, 2018.

[Dang *et al.*, 2020] Hao Dang, Feng Liu, Joel Stehouwer, Xiaoming Liu, and Anil K Jain. On the detection of digital face manipulation. In *CVPR*, 2020.

[Goodfellow *et al.*, 2014] Ian Goodfellow, Jean Pouget-Abadie, Mehdi Mirza, Bing Xu, David Warde-Farley, Sherjil Ozair, Aaron Courville, and Yoshua Bengio. Generative adversarial networks. In *NeurIPS*, 2014.

[Guan *et al.*, 2023] Jiazhi Guan, Tianshu Hu, Hang Zhou, Zhizhi Guo, Lirui Deng, Chengbin Quan, Errui Ding, and Youjian Zhao. Building an invisible shield for your portrait against deepfakes. *arXiv preprint arXiv:2305.12881*, 2023.

[Hacker *et al.*, 2023] Philipp Hacker, Andreas Engel, and Marco Mauer. Regulating chatgpt and other large generative ai models. In *ACM FAccT*, 2023.

[Hou *et al.*, 2023] Yang Hou, Qing Guo, Yihao Huang, Xiaofei Xie, Lei Ma, and Jianjun Zhao. Evading deepfake detectors via adversarial statistical consistency. In *CVPR*, 2023.

[Hu *et al.*, 2022] Juan Hu, Xin Liao, Jinwen Liang, Wenbo Zhou, and Zheng Qin. Finfer: Frame inference-based deepfake detection for high-visual-quality videos. In *AAAI*, 2022.

[Huang *et al.*, 2022] Hao Huang, Yongtao Wang, Zhaoyu Chen, Yuze Zhang, Yuheng Li, Zhi Tang, Wei Chu, Jingdong Chen, Weisi Lin, and Kai-Kuang Ma. Cmua-watermark: A cross-model universal adversarial watermark for combating deepfakes. In *AAAI*, 2022.

[Ilyas *et al.*, 2019] Andrew Ilyas, Shibani Santurkar, Dimitris Tsipras, Logan Engstrom, Brandon Tran, and Aleksander Madry. Adversarial examples are not bugs, they are features. In *NeurIPS*, 2019.

[Jia *et al.*, 2021] Zhaoyang Jia, Han Fang, and Weiming Zhang. Mbrs: Enhancing robustness of dnn-based watermarking by mini-batch of real and simulated jpeg compression. In *ACM MM*, 2021.

[Jolicoeur-Martineau, 2019] Alexia Jolicoeur-Martineau. The relativistic discriminator: a key element missing from standard gan. In *ICLR*, 2019.

[Juefei-Xu *et al.*, 2022] Felix Juefei-Xu, Run Wang, Yihao Huang, Qing Guo, Lei Ma, and Yang Liu. Countering malicious deepfakes: Survey, battleground, and horizon. *IJCV*, 2022.

[Karras *et al.*, 2018] Tero Karras, Timo Aila, Samuli Laine, and Jaakko Lehtinen. Progressive growing of gans for improved quality, stability, and variation. In *ICLR*, 2018.

[Karras *et al.*, 2019] Tero Karras, Samuli Laine, and Timo Aila. A style-based generator architecture for generative adversarial networks. In *CVPR*, 2019.

[Li *et al.*, 2021] Dongze Li, Wei Wang, Hongxing Fan, and Jing Dong. Exploring adversarial fake images on face manifold. In *CVPR*, 2021.

[Liang *et al.*, 2023] Chumeng Liang, Xiaoyu Wu, Yang Hua, Jiaru Zhang, Yiming Xue, Tao Song, Zhengui Xue, Ruhui Ma, and Haibing Guan. Adversarial example does good: Preventing painting imitation from diffusion models via adversarial examples. In *ICML*, 2023.

[Lin *et al.*, 2022] Yuzhen Lin, Han Chen, Emanuele Maiorana, Patrizio Campisi, and Bin Li. Source-id-tracker: Source face identity protection in face swapping. In *ICME*, 2022.

[Liu *et al.*, 2022] Xinwei Liu, Jian Liu, Yang Bai, Jindong Gu, Tao Chen, Xiaojun Jia, and Xiaochun Cao. Watermark vaccine: Adversarial attacks to prevent watermark removal. In *ECCV*, 2022.

[Liu *et al.*, 2023] Honggu Liu, Xiaodan Li, Wenbo Zhou, Han Fang, Paolo Bestagini, Weiming Zhang, Yuefeng Chen, Stefano Tubaro, Nenghai Yu, Yuan He, et al. Bifpro: A bidirectional facial-data protection framework against deepfake. In *ACM MM*, 2023.

[Neekhara *et al.*, 2022] Paarth Neekhara, Shehzeen Hussain, Xinqiao Zhang, Ke Huang, Julian McAuley, and Farinaz Koushanfar. Facesigns: semi-fragile neural watermarks for media authentication and countering deepfakes. *arXiv preprint arXiv:2204.01960*, 2022.

[Ojha *et al.*, 2023] Utkarsh Ojha, Yuheng Li, and Yong Jae Lee. Towards universal fake image detectors that generalize across generative models. In *CVPR*, 2023.

[Poursaeed *et al.*, 2018] Omid Poursaeed, Isay Katsman, Bicheng Gao, and Serge Belongie. Generative adversarial perturbations. In *CVPR*, 2018.

[Rossler *et al.*, 2019] Andreas Rossler, Davide Cozzolino, Luisa Verdoliva, Christian Riess, Justus Thies, and Matthias Nießner. Faceforensics++: Learning to detect manipulated facial images. In *ICCV*, 2019.

[Shiohara and Yamasaki, 2022] Kaede Shiohara and Toshihiko Yamasaki. Detecting deepfakes with self-blended images. In *CVPR*, 2022.

[Siarohin *et al.*, 2019] Aliaksandr Siarohin, Stéphane Lathuilière, Sergey Tulyakov, Elisa Ricci, and Nicu Sebe. First order motion model for image animation. In *NeurIPS*, 2019.

[Sun *et al.*, 2022a] Pu Sun, Yuezun Li, Honggang Qi, and Siwei Lyu. Faketracer: Exposing deepfakes with training data contamination. In *ICIP*, 2022.

[Sun *et al.*, 2022b] Shangquan Sun, Wenqi Ren, Tao Wang, and Xiaochun Cao. Rethinking image restoration for object detection. In *NeurIPS*, 2022.

[Szegedy *et al.*, 2014] Christian Szegedy, Wojciech Zaremba, Ilya Sutskever, Joan Bruna, Dumitru Erhan, Ian Goodfellow, and Rob Fergus. Intriguing properties of neural networks. In *ICLR*, 2014.

[Tancik *et al.*, 2020] Matthew Tancik, Ben Mildenhall, and Ren Ng. Stegastamp: Invisible hyperlinks in physical photographs. In *CVPR*, 2020.

[Wang and Deng, 2021] Chengrui Wang and Weihong Deng. Representative forgery mining for fake face detection. In *CVPR*, 2021.

[Wang *et al.*, 2020] Sheng-Yu Wang, Oliver Wang, Richard Zhang, Andrew Owens, and Alexei A Efros. Cnn-generated images are surprisingly easy to spot... for now. In *CVPR*, 2020.

[Wang *et al.*, 2021] Run Wang, Felix Juefei-Xu, Meng Luo, Yang Liu, and Lina Wang. Faketagger: Robust safeguards against deepfake dissemination via provenance tracking. In *ACM MM*, 2021.

[Wang *et al.*, 2022a] Run Wang, Ziheng Huang, Zhikai Chen, Li Liu, Jing Chen, and Lina Wang. Anti-forgery: Towards a stealthy and robust deepfake disruption attack via adversarial perceptual-aware perturbations. In *IJCAI*, 2022.

[Wang *et al.*, 2022b] Xueyu Wang, Jiajun Huang, Siqi Ma, Surya Nepal, and Chang Xu. Deepfake disrupter: The detector of deepfake is my friend. In *CVPR*, 2022.

[Wang *et al.*, 2023] Tianyi Wang, Mengxiao Huang, Harry Cheng, Bin Ma, and Yinglong Wang. Robust identity perceptual watermark against deepfake face swapping. *arXiv preprint arXiv:2311.01357*, 2023.

[Wu *et al.*, 2023] Xiaoshuai Wu, Xin Liao, and Bo Ou. Sepmark: Deep separable watermarking for unified source tracing and deepfake detection. In *ACM MM*, 2023.

[Xiao *et al.*, 2018] Chaowei Xiao, Bo Li, Jun-Yan Zhu, Warren He, Mingyan Liu, and Dawn Song. Generating adversarial examples with adversarial networks. In *IJCAI*, 2018.

[Xie *et al.*, 2020] Cihang Xie, Mingxing Tan, Boqing Gong, Jiang Wang, Alan L Yuille, and Quoc V Le. Adversarial examples improve image recognition. In *CVPR*, 2020.

[Xiong *et al.*, 2023] Cheng Xiong, Chuan Qin, Guorui Feng, and Xinpeng Zhang. Flexible and secure watermarking for latent diffusion model. In *ACM MM*, 2023.

[Yu *et al.*, 2021] Ning Yu, Vladislav Skripniuk, Sahar Abdelnabi, and Mario Fritz. Artificial fingerprinting for generative models: Rooting deepfake attribution in training data. In *ICCV*, 2021.

[Yu *et al.*, 2023] Chong Yu, Tao Chen, and Zhongxue Gan. Adversarial amendment is the only force capable of transforming an enemy into a friend. In *IJCAI*, 2023.

[Zhang *et al.*, 2018] Richard Zhang, Phillip Isola, Alexei A Efros, Eli Shechtman, and Oliver Wang. The unreasonable effectiveness of deep features as a perceptual metric. In *CVPR*, 2018.

[Zhang *et al.*, 2024a] Xuanyu Zhang, Runyi Li, Jiwen Yu, Youmin Xu, Weiqi Li, and Jian Zhang. Editguard: Versatile image watermarking for tamper localization and copyright protection. In *CVPR*, 2024.

[Zhang *et al.*, 2024b] Yunming Zhang, Dengpan Ye, Caiyun Xie, Long Tang, Xin Liao, Ziyi Liu, Chuanxi Chen, and Jiacheng Deng. Dual defense: Adversarial, traceable, and invisible robust watermarking against face swapping. *IEEE TIFS*, 2024.

[Zhao *et al.*, 2021] Hanqing Zhao, Wenbo Zhou, Dongdong Chen, Tianyi Wei, Weiming Zhang, and Nenghai Yu. Multi-attentional deepfake detection. In *CVPR*, 2021.

[Zhao *et al.*, 2023a] Xuandong Zhao, Kexun Zhang, Yu-Xiang Wang, and Lei Li. Generative autoencoders as watermark attackers: Analyses of vulnerabilities and threats. *arXiv preprint arXiv:2306.01953*, 2023.

[Zhao *et al.*, 2023b] Yuan Zhao, Bo Liu, Ming Ding, Baoping Liu, Tianqing Zhu, and Xin Yu. Proactive deepfake defence via identity watermarking. In *WACV*, 2023.

[Zhao *et al.*, 2023c] Zhengyu Zhao, Hanwei Zhang, Renjue Li, Ronan Sicre, Laurent Amsaleg, Michael Backes, Qi Li, and Chao Shen. Revisiting transferable adversarial image examples: Attack categorization, evaluation guidelines, and new insights. *arXiv preprint arXiv:2310.11850*, 2023.

[Zhu *et al.*, 2018] Jiren Zhu, Russell Kaplan, Justin Johnson, and Li Fei-Fei. Hidden: Hiding data with deep networks. In *ECCV*, 2018.

[Zhu *et al.*, 2023] Yao Zhu, Yuefeng Chen, Xiaodan Li, Rong Zhang, Xiang Tian, Bolun Zheng, and Yaowu Chen. Information-containing adversarial perturbation for combating facial manipulation systems. *IEEE TIFS*, 2023.